

Spin Fluctuation Induced Superconductivity Controlled by Orbital Fluctuation

T Takimoto[†], T Hotta[†], T Maehira[†], and K Ueda[‡]

[†] *Advanced Science Research Center, Japan Atomic Energy Research Institute, Tokai, Ibaraki 319-1195, Japan*

[‡] *Institute for Solid State Physics, University of Tokyo, 5-1-5 Kashiwa-no-ha, Kashiwa, Chiba 277-8581, Japan*

(October 31, 2018)

A microscopic Hamiltonian reflecting the correct symmetry of f -orbitals is proposed to discuss superconductivity in heavy fermion systems. In the orbitally degenerate region in which not only spin fluctuations but also orbital fluctuations develop considerably, cancellation between spin and orbital fluctuations destabilizes $d_{x^2-y^2}$ -wave superconductivity. Entering the non-degenerate region by increasing the crystalline electric field, $d_{x^2-y^2}$ -wave superconductivity mediated by antiferromagnetic spin fluctuations emerges out of the suppression of orbital fluctuations. We argue that the present scenario can be applied to recently discovered superconductors CeTIn₅ (T=Ir, Rh, and Co).

Unconventional superconductivity has been one of central issues in the research field of strongly correlated electron systems. Especially since the discovery of high temperature superconductivity in cuprates, much effort has been focussed on elucidating the mechanism of unconventional superconductivity, clarifying that a crucial role is played by antiferromagnetic (AF) “spin fluctuations” (SF) [1]. The importance of AFSF is widely recognized, for instance, in $4f$ - and $5f$ -electron superconducting materials such as CeCu₂Si₂ [2] and UPd₂Al₃ [3] as well as in organic superconductors such as κ -(BEDT-TTF) [4]. Thus, it is widely believed that a broad class of unconventional superconductors originates from SF.

In d - and f -electron systems, however, the potential importance of *orbital* degrees of freedom has recently been discussed intensively. In fact, “orbital ordering” is found to be a key issue for understanding microscopic aspects of the charge-ordered phase in colossal magnetoresistive manganites [5]. This orbital ordering is primarily relevant to the insulating phase, while “orbital fluctuations” (OF) should be significant in the metallic phase. Recently, the effects of OF have attracted attention, since it is hoped to provide a new scenario for superconductivity [6]. Especially from a conceptual viewpoint, it is important to clarify how superconductivity emerges when both SF and OF play active roles.

As a typical material for investigating superconductivity in a system with both SF and OF, let us introduce the recently discovered heavy-fermion superconductors CeTIn₅ (T=Ir, Rh, and Co) [7] with the HoCoGa₅-type tetragonal crystal structure. Due to this structure and to strong correlation effects, the similarity with cuprates has been emphasized. In particular, AFSF also plays an essential role in the Ce-115 system, since it exhibits quasi two-dimensional Fermi surfaces [8] and the AF phase exists next to the superconducting state in the phase diagram of CeRh_{1-x}Ir_xIn₅ [9]. In fact, a line node in the gap function has been observed in CeTIn₅ by various experimental techniques [10]. It may be true that superconductivity itself is due to AFSF, but an important role for the OF has been overlooked in spite of the fact that both SF and OF are originally included in the ground-state

multiplet of Ce³⁺ ion. In actual materials, superconductivity occurs in a situation where OF is suppressed, since orbital degeneracy is lifted by the effect of the crystalline electric field (CEF). Thus, we envision a scenario where OF controls the stability of the superconductivity even though it originates from AFSF.

In this Letter, we investigate superconductivity based on the orbitally degenerate Hubbard model constructed by the tight-binding method [11]. Solving the gap equation with the pairing interaction evaluated using the random phase approximation (RPA), we obtain several superconducting phases around the spin and orbital ordered phases. In the orbitally degenerate region where both SF and OF are developed, it is found that singlet superconductivity is suppressed due to the competition between them, while triplet superconductivity is favored since they are cooperative in this case. When a level splitting is included to lift the orbital degeneracy, $d_{x^2-y^2}$ -wave superconductivity due to AFSF is stabilized in the vicinity of the AF phase. Thus, we claim that AFSF-induced superconductivity in Ce-115 systems is substantiated in consequence of the suppression of OF.

In order to construct the microscopic model for f -electron systems, let us start our discussion from a local basis of the Ce³⁺ ion. Among the 14-fold degenerate $4f$ -electron states, due to the effect of strong spin-orbit coupling, only the $j=5/2$ sextuplet effectively contributes to the low-energy excitations (j is total angular momentum). This sextuplet is further split into a Γ_7 doublet and a Γ_8 quadruplet due to the effect of cubic CEF, where the eigen states are given by $|\Gamma_{7\pm}\rangle = \sqrt{1/6}|\pm 5/2\rangle - \sqrt{5/6}|\mp 3/2\rangle$, $|\Gamma_{8\pm}^{(1)}\rangle = \sqrt{5/6}|\pm 5/2\rangle + \sqrt{1/6}|\mp 3/2\rangle$, and $|\Gamma_{8\pm}^{(2)}\rangle = |\pm 1/2\rangle$. Here + and - in the subscripts denote “pseudo-spin” up and down, respectively, within each Kramers doublet.

Now we discuss the relative positions of the energy levels of Γ_7 and $\Gamma_8^{(\tau)}$ while taking account of certain features of CeTIn₅. Since CeTIn₅ has a tetragonal crystal structure and a quasi two-dimensional Fermi surface [8], it is natural to consider a two-dimensional square lattice composed of Ce ions. Due to the effect of anions surrounding

the Ce ion, it is deduced that the energy level of Γ_7 becomes higher than those of Γ_8 's. Thus, in the following, the Γ_7 orbital is neglected for simplicity. Note also that we need to include the effect of the tetragonal CEF, which lifts the degeneracy of the $\Gamma_8^{(\tau)}$. Although a mixing between Γ_7 and $\Gamma_8^{(1)}$ generally occurs under a tetragonal CEF, such a mixing is expected to be small since the Γ_7 orbital has higher energy. Thus, in this situation, the effect of a tetragonal CEF can be included in terms of a level splitting ε between the $\Gamma_8^{(1)}$ and $\Gamma_8^{(2)}$ orbitals. In order to explain the magnetic anisotropy observed in experiments, $\Gamma_8^{(1)}$ must be lower than $\Gamma_8^{(2)}$, i.e., $\varepsilon > 0$ in CeTlIn₅. The magnitude of ε for each CeTlIn₅ compound will be discussed later. It should be noted that the above level scheme is consistent with the following two facts: (i) Experimental results for CeTlIn₅ exhibit a larger uniform susceptibility for magnetic field perpendicular to the CeIn₃ plane than for the parallel case [7,12]. This significant anisotropy is well explained under the assumption that Γ_7 is *not* the lowest-energy state and ε is *positive*. (ii) The band-structure calculation results suggest that the almost flat band corresponding to Γ_7 appears above the Fermi level [11].

In order to include the itinerant features of the $4f$ -electrons, a simple way is to include nearest-neighbor hopping for the f -electrons by the tight-binding method [11,13]. Although the hybridization with the In $5p$ electronic states may be important, here such an effect is considered as renormalization of the effective hopping amplitude of f -quasiparticles. Further, by adding the on-site Coulomb interaction terms among the f -electrons, the Hamiltonian becomes

$$H = \sum_{\mathbf{i}\mathbf{a}\tau\tau'\sigma} t_{\tau\tau'}^{\mathbf{a}} f_{\mathbf{i}\tau\sigma}^\dagger f_{\mathbf{i}+\mathbf{a}\tau'\sigma} - \varepsilon \sum_{\mathbf{i}} (n_{\mathbf{i}1\sigma} - n_{\mathbf{i}2\sigma})/2 + U \sum_{\mathbf{i}\tau} n_{\mathbf{i}\tau\uparrow} n_{\mathbf{i}\tau\downarrow} + U' \sum_{\mathbf{i}\sigma\sigma'} n_{\mathbf{i}1\sigma} n_{\mathbf{i}2\sigma'}, \quad (1)$$

where $f_{\mathbf{i}\tau\sigma}$ is the annihilation operator for an f -electron with pseudo-spin σ in the orbital $\Gamma_8^{(\tau)}$ at site \mathbf{i} , \mathbf{a} is the vector connecting nearest-neighbor sites, and $n_{\mathbf{i}\tau\sigma} = f_{\mathbf{i}\tau\sigma}^\dagger f_{\mathbf{i}\tau\sigma}$. The first term represents the nearest-neighbor hopping of f -electrons with the amplitude $t_{\tau\tau'}^{\mathbf{a}}$ between $\Gamma_8^{(\tau)}$ and $\Gamma_8^{(\tau')}$ along the \mathbf{a} -direction, given by $t_{11}^{\mathbf{x}} = -\sqrt{3}t_{12}^{\mathbf{x}} = -\sqrt{3}t_{21}^{\mathbf{x}} = 3t_{22}^{\mathbf{x}} = 1$ for $\mathbf{a}=\mathbf{x}$ and $t_{11}^{\mathbf{y}} = \sqrt{3}t_{12}^{\mathbf{y}} = \sqrt{3}t_{21}^{\mathbf{y}} = 3t_{22}^{\mathbf{y}} = 1$ for $\mathbf{a}=\mathbf{y}$, respectively, in energy units where $t_{11}^{\mathbf{x}} = 1$. Note the positive sign of the first term in H , since the M-point, not the Γ -point, is at the bottom of the bands forming the Fermi surfaces [11]. Note also that the present $t_{\tau\tau'}^{\mathbf{a}}$ is just the same as that of the e_g electrons [5], but this point will be discussed elsewhere. The second term denotes the tetragonal CEF. In the third and fourth terms, U and U' are the intra- and inter-orbital Coulomb interactions, respectively. In reality, $U=U'$, since they originate from the same Coulomb interactions among f -orbitals in the $j=5/2$ multiplet, but in this paper, we also treat the case where $U \neq U'$ in order to analyze the roles

of SF and OF. Since we consider quarter-filling (one f -electron per site), the model in the limit of $\varepsilon=\infty$ reduce to the half-filled, single-orbital Hubbard model.

Now, in order to investigate superconductivity around the spin and/or orbital ordered phases, we calculate spin and orbital susceptibilities, $\hat{\chi}^s(\mathbf{q})$ and $\hat{\chi}^o(\mathbf{q})$, respectively. Within the RPA, these are given in a matrix form as

$$\hat{\chi}^s(\mathbf{q}) = [\hat{1} - \hat{U}^s \hat{\chi}(\mathbf{q})]^{-1} \hat{\chi}(\mathbf{q}), \quad (2)$$

$$\hat{\chi}^o(\mathbf{q}) = [\hat{1} + \hat{U}^o \hat{\chi}(\mathbf{q})]^{-1} \hat{\chi}(\mathbf{q}), \quad (3)$$

where labels of row and column in the matrix appear in the order 11, 22, 12, and 21, these being pairs of orbital indices 1 and 2. Note that $\hat{1}$ is the 4×4 unit matrix. \hat{U}^s is given by $U_{11,11}^s = U_{22,22}^s = U$, $U_{12,12}^s = U_{21,21}^s = U'$, otherwise zero, while \hat{U}^o is expressed as $U_{11,11}^o = U_{22,22}^o = U$, $U_{11,22}^o = U_{22,11}^o = 2U'$, $U_{12,12}^o = U_{21,21}^o = -U'$, otherwise zero. The matrix elements of $\hat{\chi}(\mathbf{q})$ are defined by $\chi_{\mu\nu,\alpha\beta}(\mathbf{q}) = -T \sum_{\mathbf{k},n} G_{\alpha\mu}^{(0)}(\mathbf{k}+\mathbf{q}, i\omega_n) G_{\nu\beta}^{(0)}(\mathbf{k}, i\omega_n)$, where T is temperature, $G_{\mu\nu}^{(0)}(\mathbf{k}, i\omega_n)$ is the non-interacting Green's function for f -electrons with momentum \mathbf{k} propagating between μ - and ν -orbitals, and $\omega_n = \pi T(2n+1)$ with integer n . The instabilities for the spin- and orbital-ordered phases are determined by the conditions of $\det[\hat{1} - \hat{U}^s \hat{\chi}(\mathbf{q})] = 0$ and $\det[\hat{1} + \hat{U}^o \hat{\chi}(\mathbf{q})] = 0$, respectively.

By using $\hat{\chi}^s(\mathbf{q})$ and $\hat{\chi}^o(\mathbf{q})$, the superconducting gap equation is given as

$$\Delta^\xi(\mathbf{k}) = \sum_{\mathbf{k}'} \hat{V}^\xi(\mathbf{k} - \mathbf{k}') \hat{\phi}(\mathbf{k}') \Delta^\xi(\mathbf{k}'), \quad (4)$$

where $\Delta^\xi(\mathbf{k}) = [\Delta_{11}^\xi(\mathbf{k}), \Delta_{22}^\xi(\mathbf{k}), \Delta_{12}^\xi(\mathbf{k}), \Delta_{21}^\xi(\mathbf{k})]^t$ is the gap function in the vector representation for a singlet ($\xi = S$) or triplet ($\xi = T$) pairing state, and the matrix elements of the singlet- and triplet-pairing potentials, respectively, are given by

$$V_{\alpha\beta,\mu\nu}^S(\mathbf{q}) = [(-3/2)\hat{W}^s(\mathbf{q}) + (1/2)\hat{W}^o(\mathbf{q}) + \hat{U}^s]_{\alpha\mu,\nu\beta}, \quad (5)$$

$$V_{\alpha\beta,\mu\nu}^T(\mathbf{q}) = [(1/2)\hat{W}^s(\mathbf{q}) + (1/2)\hat{W}^o(\mathbf{q}) - \hat{U}^s]_{\alpha\mu,\nu\beta}. \quad (6)$$

Here, the spin and orbital susceptibilities are included as $\hat{W}^s(\mathbf{q}) = \hat{U}^s + \hat{U}^s \hat{\chi}^s(\mathbf{q}) \hat{U}^s$ and $\hat{W}^o(\mathbf{q}) = -\hat{U}^o + \hat{U}^o \hat{\chi}^o(\mathbf{q}) \hat{U}^o$. The elements of the pair correlation function $\hat{\phi}(\mathbf{k})$ are given by $\phi_{\alpha\beta,\mu\nu}(\mathbf{k}) = T \sum_n G_{\alpha\mu}^{(0)}(\mathbf{k}, -i\omega_n) G_{\nu\beta}^{(0)}(-\mathbf{k}, i\omega_n)$. The superconducting transition is obtained for each respective irreducible representation by solving Eq. (4), where the maximum eigenvalue becomes unity.

Here we mention the essential symmetries of the Cooper pairs in multi-orbital systems. The pairing states are classified into four types owing to spin $SU(2)$ symmetry and space inversion symmetry; (1) spin-singlet and orbital-symmetric with even-parity, (2) spin-triplet and orbital-symmetric with odd-parity, (3) spin-singlet and orbital-antisymmetric with odd-parity, and (4) spin-triplet and orbital-antisymmetric with even-parity. Note that $SU(2)$ symmetry does not exist in orbital space,

since the lattice and the local wavefunctions rotate simultaneously. For (1) and (2), f -electrons in the same band form the Cooper pair, while for (3) and (4), such a pair is formed only between different bands. Except for the special case in which two Fermi surfaces connect with each other, orbital-antisymmetric pairing is unstable due to depairing effects destroy inter-band pairs. In fact, even after careful calculations, we do not find any region for (3) and (4) in the parameter space considered here. Thus, in the following, we discuss only the orbital-symmetric pair.

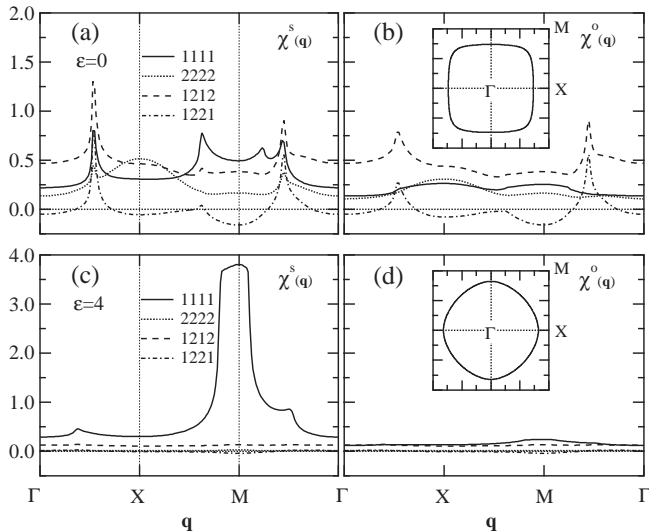


FIG. 1. (a) Spin and (b) orbital susceptibilities in \mathbf{q} space for $\varepsilon=0$ and $U=U'=0.9U_m$. (c) and (d) are for $\varepsilon=4$. Insets indicate the Fermi-surface lines.

Let us discuss first the effect of ε on the correlation between SF and OF. Since we are considering a realistic situation corresponding to CeTIn_5 , we restrict ourselves to the case of $U=U'$ for a while. In Fig. 1, the principal components of $\hat{\chi}^s(\mathbf{q})$ and $\hat{\chi}^o(\mathbf{q})$ are shown in \mathbf{q} space for $U=U'=0.9U_m$, where U_m denotes spin instability determined from $\det[\hat{1} - \hat{U}^s \hat{\chi}(\mathbf{q})] = 0$. In the orbital-degenerate case with $\varepsilon=0$, as shown in Figs. 1(a) and (b), the overall magnitude of OF is comparable with that of SF. As for the \mathbf{q} dependence, common structures are found in $\chi^s(\mathbf{q})$ and $\chi^o(\mathbf{q})$. Namely, there are two peaks around $(\pi/2, \pi/2)$ and $(\pi/2, 0)$ owing to the nesting properties of the Fermi surface (see the inset). Thus, the orbital-degenerate region is characterized by competition between SF and OF. With increasing ε , the Fermi surface approaches a shape having the nesting vector (π, π) (see the inset). For $\varepsilon=4$, as shown in Fig. 1(c) and (d), OF is almost completely suppressed, and SF around (π, π) become dominant. Note here that the increase of ε makes the lower energy state favorable and suppresses excitations to the upper energy state, indicating the suppression of OF. Thus, even at this stage, it is understood that the suppression of OF leads to the development of SF for the paramagnetic system which is wavering between spin-

and orbital-ordering.

Next, we consider how a superconducting phase emerges when ε is increased. In Fig. 2(a), the maximum eigenvalues for several irreducible representations are depicted as a function of ε for $U=U'=2.5$. The calculations are carried out for a fixed $T=0.02$, and the first Brillouin zone is divided into 128×128 meshes. In the orbital-degenerate region, several eigenvalues are very close to each other owing to multi-peak structures in $\hat{\chi}^s(\mathbf{q})$ and $\hat{\chi}^o(\mathbf{q})$. With increasing ε , as is easily understood from the growth of AFSF mentioned above, the eigenvalue for B_{1g} symmetry becomes dominant and finally at $\varepsilon \approx 3$, the B_{1g} superconducting phase is stabilized. On further increasing ε , the AF instability eventually occurs, since the system asymptotically approaches the half-filled single-orbital Hubbard model. We emphasize that the increase of ε brings transitions successively in the order of PM, B_{1g} superconducting, and AF phases.

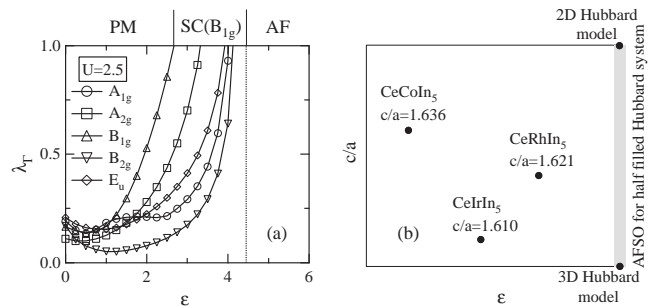


FIG. 2. (a) Maximum eigenvalue vs. ε for the respective irreducible representation at $U=U'=2.5$. (b) Schematic plot c/a vs. ε to illustrate a comparison between our theory and actual CeTIn_5 compounds.

Based on the above calculated results, let us try to explain the differences among three Ce-115 compounds, CeRhIn_5 (Néel temperature $T_N=3.8\text{K}$), CeIrIn_5 (superconducting transition temperature $T_c=0.4\text{K}$), and CeCoIn_5 ($T_c=2.3\text{K}$) [7]. One property which distinguishes these compounds is two-dimensionality, as expressed by the ratio c/a between lattice constants. It is naturally expected that two-dimensionality becomes stronger in the order of CeIrIn_5 , CeRhIn_5 , and CeCoIn_5 [7]. Since the magnetic state should be stabilized with increasing three-dimensionality, CeIrIn_5 should be most favorable for the occurrence of antiferromagnetism among three compounds, but this is obviously inconsistent with experimental results. This inconsistency is resolved by introducing another important ingredient ε . One can show that the increase of magnetic anisotropy just corresponds to the increase of ε . Analysis of experimental results for the anisotropy of magnetic susceptibilities [7,12] leads to the conclusion that ε becomes larger in the order of CeCoIn_5 , CeIrIn_5 , and CeRhIn_5 . Taking into account the effect of ε in addition to dimensionality, we arrive at the picture schematically shown in Fig. 2(b). Due to the enhancement of AFSF induced by increasing ε , as shown in Fig. 1, it may be understood that CeRhIn_5

rather than CeIrIn₅ is more favorable to antiferromagnetism. Namely, it is considered that CeRhIn₅ with the largest ε is antiferromagnet, while CeCoIn₅ and CeIrIn₅ with smaller ε than CeRhIn₅ exhibit superconductivity. The difference in T_c between CeCoIn₅ and CeIrIn₅ may be attributed to the extent of two-dimensionality. Concerning the superconductivity and antiferromagnetism of CeTiIn₅ compounds, the combination of two dimensionality and the crystalline field splitting is necessary to reach a consistent picture.

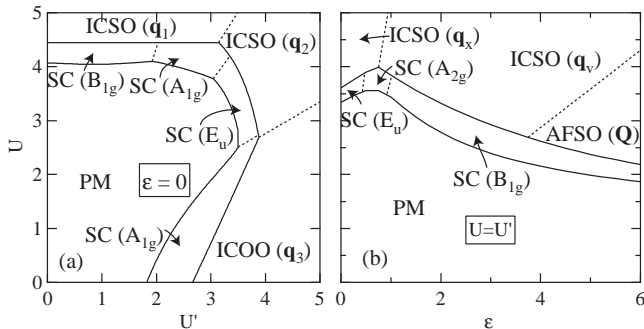


FIG. 3. Phase diagram (a) in the U - U' plane for $\varepsilon=0$ and (b) in the U - ε plane for $U=U'$. Meanings of abbreviations used here are as follows: SC(Γ) denotes superconducting phase with Γ -symmetry, ICSO(\mathbf{q}) indicates incommensurate spin ordered phase with wave vector \mathbf{q} , ICOO(\mathbf{q}) is incommensurate orbital ordered phase with wave vector \mathbf{q} , and AFSO(\mathbf{Q}) denotes antiferromagnetic spin ordered phase. Several wave vectors are defined as $\mathbf{q}_1=(0.56\pi, 0.56\pi)$, $\mathbf{q}_2=(0.53\pi, 0)$, $\mathbf{q}_3=(\pi, 0)$, $\mathbf{q}_x=(q_x, 0)$, $\mathbf{q}_y=(\pi, q_y)$, and $\mathbf{Q}=(\pi, \pi)$. Solid curves are the phase boundaries determined by actual calculations, while dotted lines are schematic phase boundary guides for the eye.

The orbitally degenerate model, Eq. (1), shows new, rich superconducting properties both for singlet and triplet pairings. In Fig. 3(a) and (b), we show the phase diagrams in the U - U' plane for $\varepsilon=0$ and U - ε plane for $U=U'$, respectively. In these figures, four characteristic superconducting phases are observed: (1) a SF-mediated spin-singlet superconducting phase with B_{1g} -symmetry in the vicinity of a spin-ordered phase; (2) a g -wave superconducting phase with A_{2g} -symmetry; (3) a spin-triplet superconducting phase with E_u -symmetry due to the cooperation between SF and OF around $U=U'$ and $\varepsilon=0$ and (4) an OF-mediated spin-singlet superconducting phase with A_{1g} -symmetry for $U \ll U'$ around an orbital-ordered phase. With respect to (1), it is thought that B_{1g} -superconductivity is induced by SF around $\mathbf{q}=\mathbf{Q}=(\pi, \pi)$. Concerning the triplet superconductivity (3), note that for this region all superconducting instabilities are quite close to each other because of the multi-peak structures in $\hat{\chi}^s(\mathbf{q})$ and $\hat{\chi}^o(\mathbf{q})$ as shown in Fig. 1. We also note that the factors in front of the SF term in $\hat{W}^s(\mathbf{q})$ are $-3/2$ for singlet and $+1/2$ for triplet pairing, while the factor for the OF term in $\hat{W}^o(\mathbf{q})$ is $+1/2$ for both pairings. Namely, OF is cooperative with SF for

spin-triplet pairing, while SF and OF compete with each other for spin-singlet pairing [6]. Thus, the spin-triplet pairing phase appears in the region for $\varepsilon \approx 0$ and $U \approx U'$. The mechanism of the OF-mediated singlet superconductivity (4) is interesting. In this state, two quasi-particles with different pseudo-spin form an on-site intra-orbital singlet pair since $U' \gg U$, leading to A_{1g} superconductivity. In short, singlet superconductivity with B_{1g} - or A_{1g} -symmetry is stabilized when either SF or OF is dominant, while triplet superconductivity is favored when there is cooperation between SF and OF.

In summary, we have studied superconductivity in the Ce-115 systems based on the orbitally degenerate Hubbard model, and found that with increasing the tetragonal CEF splitting $d_{x^2-y^2}$ -wave superconductivity due to AFSF emerges out of the suppression of OF in the vicinity of the AF phase. The concept of AFSF-induced superconductivity controlled by OF qualitatively explains the difference among Ce-115 materials.

The authors thank H. Harima, A. Hasegawa, T. Moriya, Y. Ōnuki, R. E. Walstedt, and K. Yamada for discussions. K.U. is financially supported by Grant-in-Aid for Scientific Research Areas (B) from the Ministry of Education, Science, Sports, Culture, and Technology.

-
- [1] Scalapino D J 1995 *Phys. Rep.* **250** 329
 - Moriya T and Ueda K 2000 *Adv. Phys.* **49** 555
 - [2] Steglich F *et al.* 1979 *Phys. Rev. Lett.* **43** 1892
 - [3] Geibel C *et al.* 1991 *Z. Phys. B* **84** 1
 - [4] Jérôme D and Schulz H J 1982 *Adv. Phys.* **31** 299
 - [5] Dagotto E, Hotta T, and Moreo A 2001 *Phys. Rep.* **344** 1 and references therein
 - [6] Takimoto T 2000 *Phys. Rev. B* **62** R14641
 - [7] Hegger H *et al.* 2000 *Phys. Rev. Lett.* **84** 4986
 - Petrovic C *et al.* 2001 *Europhys. Lett.* **53** 354
 - Petrovic C *et al.* 2001 *J. Phys.: Condens. Matter* **13** L337
 - [8] Haga Y *et al.* 2001 *Phys. Rev. B* **63** R060503
 - Settai R *et al.* 2001 *J. Phys.: Condens. Matter.* **13** L627
 - [9] Pagliuso P G *et al.* 2001 *Phys. Rev. B* **64** R100503
 - [10] Kohori Y *et al.* 2000 *Eur. Phys. J. B* **18** 601
 - Zheng G-q *et al.* 2001 *Phys. Rev. Lett.* **86** 4664
 - Movshovich R *et al.* 2001 *Phys. Rev. Lett.* **86** 5152
 - Izawa K *et al.* 2001 *Phys. Rev. Lett.* **87** 057002
 - [11] Maehira T *et al.* to appear in *J. Phys. Soc. Jpn.*
 - [12] Takeuchi T *et al.* 2001 *J. Phys. Soc. Jpn.* **70** 877
 - [13] Takegahara K *et al.* 1980 *J. Phys. C: Solid St. Phys.* **13** 583 and references therein